IC/92/53

INTERNATIONAL CENTRE FOR THEORETICAL PHYSICS

HIGH-TEMPERATURE MORPHOLOGY OF STEPPED GOLD SURFACES

G. Bilalbegović

F. Ercolessi

and

E. Tosatti

INTERNATIONAL ATOMIC ENERGY AGENCY

UNITED NATIONS EDUCATIONAL, SCIENTIFIC AND CULTURAL ORGANIZATION

MIRAMARE-TRIESTE

International Atomic Energy Agency
and
United Nations Educational Scientific and Cultural Organization
INTERNATIONAL CENTRE FOR THEORETICAL PHYSICS

HIGH-TEMPERATURE MORPHOLOGY OF STEPPED GOLD SURFACES

G. Bilalbegović
International Centre for Theoretical Physics, Trieste, Italy
and
International School for Advanced Studies, Trieste, Italy,

F. Ercolessi
International School for Advanced Studies, Trieste, Italy,

and

E. Tosatti
International Centre for Theoretical Physics, Trieste, Italy
and
International School for Advanced Studies, Trieste, Italy.

MIRAMARE – TRIESTE
April 1992

Molecular dynamics simulations with a classical many–body potential are used to study the high–temperature stability of stepped non–melting metal surfaces. We have studied in particular the Au(111) vicinal surfaces in the $(M+1, M-1, M)$ family and the Au(100) vicinals in the $(M,1,1)$ family. Some vicinal orientations close to the non–melting Au(111) surface become unstable close to the bulk melting temperature and facet into a mixture of crystalline (111) regions and localized surface–melted regions. On the contrary, we do not find high–temperature faceting for vicinals close to Au(100), also a non–melting surface. These (100) vicinal surfaces gradually disorder with disappearance of individual steps well below the bulk melting temperature. We have also studied the high–temperature stability of ledges formed by pairs of monoatomic steps of opposite sign on the Au(111) surface. It is found that these ledges attract each other, so that several of them merge into one larger ledge, whose edge steps then act as a nucleation site for surface melting.

I. INTRODUCTION

An important aspect of phase transitions at surfaces, such as roughening [1–3] and surface melting [4–6], is their anisotropy, i.e. crystal face dependence. The existence of different roughening transitions associated with the disappearance of different facets of the same crystal at different temperatures is well known. On the contrary, the anisotropy of surface melting, as well as the interplay between roughening and surface melting, although of great current interest, are considerably less understood. Since surface melting is just a specific type of wetting, this problem can be formulated as one of interrelation between roughening and wetting. Statistical mechanics studies [7–9] show that, even in the simplest models of wetting and roughening, different routes for the behavior of an interface are possible. The question of stability of surfaces is connected with the anisotropy of the surface free energy of crystals [1–3,10]. Unstable vicinal surfaces facet and evolve into hill–and–valley structures. Sharp edges are then present on the equilibrium crystal shape.

In early experimental investigations of the surface melting anisotropy for crystals, such as Cu and Au, it was found [11,12] that all faces of the hot crystal are covered with melt except for circular areas around (111) and (100) facets, which appear to remain crystalline and flat. Recent ion shadowing and blocking experiments [4,13], as well as scanning electron microscopy measurements [14–17], for Pb crystals also provide strong evidence of surface melting anisotropy. In particular, the open Pb(110) surface exhibits a very pronounced surface melting, whereas the close–packed Pb(111) does not melt. A cylindrical Pb crystal [13] reveals the existence of surface melting for many orientations, except for a well–developed band around the (111) face and, possibly also a zone around (100). Heyraud, Métois and Bermond [14–16], as well as Pavlovska, Faulien and Bauer [17], studied extensively the equilibrium shapes of lead crystals in the surface melting temperature region (some percent below T_m). They found that the junction between the non–melting (111) facet and the rounded, surface melted part of the crystal becomes sharp about $\sim 20K$ below the bulk melting point. Although a non–melting zone was found also around (100), the existence of sharp edges close to these facets remained unsolved [14–17]. Nozières recently proposed some thermodynamics arguments which suggest that surface melting close to the non–melting face may be induced by the presence of steps on vicinal surfaces [18,19]. A generalization of the Wulff construction to the temperatures near the bulk melting point was also presented [20]. Yang, Lu and Wang studied thermal stability of the stepped Pb(111) surface [21]. They found that near the bulk melting temperature surface steps appear to suddenly collapse, leaving behind a step–free, flat surface. A possible explanation could be formation of a melted drops, or steps collapse to form crystalline microfacets.

We present here a Molecular Dynamics (MD) study of the high–temperature morphology for several stepped surfaces in particular those that are vicinals of the non–melting (111) and (100) faces of gold. In Section II some details of MD simulation method are given. Our results for the Au(111) vicinal surfaces (presented in Section III) indicate how (111) vicinals are unstable near the bulk melting temperature and facet into the flat (111) region and the surface–melted region. This high–temperature melting–related faceting has been presented and discussed recently by our group [22,23]. On the contrary, the (100) vicinals in the $(M,1,1)$

family (Section V) as well as surfaces with monoatomic steps of opposite sign on Au(111) (Section IV), do not facet but show a different type of the step instability at high temperatures. Possible reasons for the different behavior of these surfaces are discussed.

II. MOLECULAR DYNAMICS SIMULATION METHOD

In order to be able to simulate correctly surface properties and phase transitions it is very important to have an accurate description of interatomic forces. It is well known that the pair potentials do not give correct description of metal surfaces and that is necessary to include many–body forces [24]. We have used here the many–body "glue" potential for Au [25]. This potential was constructed empirically, i.e. in order to reproduce some bulk gold properties and vacancy and surface formation energies. The glue Hamiltonian for gold is very well tested and gives good results for different surface properties and phase transitions, such as surface melting [26,27] and reconstruction [28,29]. We have performed MD simulations for several stepped configurations on Au(111) and Au(100). In our MD simulations for vicinal surfaces we use slabs contained by tilted MD boxes together with suitable periodic boundary conditions in two directions. Several bottom layers of the slab are kept fixed in order to mimic the infinite bulk crystal. We start from fully reconstructed surface configurations [25,26,28] at $T = 0K$ and then warm up, proceeding at each successive higher temperature from a well equilibrated configuration at the lower temperature in steps of 100K and 50K. The bulk melting temperature ($T_m \sim 1355K$) is known from previous MD simulations [25]. The

temperature of the system is controlled by rescaling particle velocities. The lattice spacing of the samples was changed with temperature according to the expansion coefficient determined in an earlier bulk simulation [25]. Depending on the sample and on the temperature our systems have been equilibrated from at least 10^4 up to 10^6 MD time steps at each temperature. The time step used in our simulations is 7.14×10^{-15} s.

III. HIGH–TEMPERATURE FACETING OF THE Au(111) VICINALS

The Au(111) surface reconstructs with an icommensurate, approximately $(23 \times \sqrt{3})$ unit cell [30,31]. Recently, the state of reconstruction on this surface was studied experimentally between 300K and 1250K and it was found that reconstruction is still present at $0.94T_m$ [31]. Circular black areas around the Au(111) facet, indicating non–melting of the Au(111) surface and a complicated behavior of vicinals around it, were found in optical emissivity measurement on crystalline gold particles [12]. Non–melting of the Au(111) surface was also found in a MD simulation study [26]. Sharp edges close to non–melting Pb(111) were recently discovered about twenty degrees below the bulk melting temperature [14–17]. We expect the existence of similar sharp edges on gold crystal shape close to Au(111) in the surface melting temperature region. Nozières presented some thermodynamic arguments [18,19] which may explain the presence of these sharp edges. The competition between melted and non–melted surface free energies produces an unstable region in the orientation of crystal faces. As is well known, a system eliminates unstable (i.e. non–convex) regions of its free energy by undergoing phase separation into

neighboring stable phases [32]. Surface faceting is precisely such a phase separation process. The origin of surface faceting may be diverse including reconstruction [29,33–37], or the presence of adsorbates [38]. Our results for the Au(534) surface presented here show that surface faceting at high temperatures is induced in this case by surface melting anisotropy on the crystal shape.

We analyse the high–temperature behavior of Au(111) vicinal surfaces of the $(M+1, M-1, M)$ family. They consist of the (111) terraces which are infinitely long along the $\langle 11\bar{2} \rangle$ direction and M atoms wide along the $\langle 1\bar{1}0 \rangle$ direction. It is important in building of MD boxes to consider the proper ABC stacking of the (111) layers in order to have a good match by periodic boundary conditions at the box boundaries. For this reason the number of steps and terraces for Au(111) vicinals must be multiple of 3, the number of (111) sublattices. After some testing we decided to model the Au(111) vicinal surfaces using MD boxes with 6 steps and 6 terraces. Although we did in fact carry out MD simulations for a number of Au(111) vicinal surfaces, a particularly detailed study was conducted for the Au(534) vicinal and only these results will be shown here as rather typical for all (111) vicinal faces. The similar behavior of the Au(423) [22], as well as a related study for the Pb(111) vicinal faces [23] were presented elsewhere.

A MD trajectory for the Au(534) surface at low temperature is shown in Fig. 1(a). This face is misoriented by 11.5° with respect to the (111) plane, and the MD box consists of 1440 particles. The same surface at a higher temperature, very close to the melting point is shown in Fig. 1(b). The steps have collapsed together to form surface liquid drops, which gives rise to the high–temperature faceting. The vicinal surface facets into crystalline, flat (111) terraces and surface–melted, droplet–like

regions. The liquid drop in Fig. 1(b) is tilted by an angle $\sim 14°$ relative to the flat face. Examples of fluctuations in Fig. 2. show that during our long simulation time (our sample have been equilibrated up to 7.5 ns) the system still fluctuates between different combinations of two phases. Such behavior is common for systems undergoing phase separation [32].

IV. BEHAVIOR OF UNLIKE STEPS AND LEDGES ON THE Au(111) SURFACE

Yang, Lu and Wang performed the high–resolution LEED study of the stepped Pb(111) surface [21]. They found that 20K below the bulk melting point steps collapse and the surface "appears to be extremely flat". We propose that the observed thermal step collapsing is due to the high–temperature faceting. The stepped surface in Ref. [21] was characterized by an average terrace width. Different stepped configurations may give the same average terrace width. Steps of the same and the opposite sign are possible on real stepped surfaces. These steps may be induced by miscuts and different types of defects and inhomogeneities during the surface preparation. Motivated by the experiment of Ref. [21] we decided to check the high–temperature stability of steps of opposite sign.

In this MD simulation the slab consists of 12 (111) layers and a total of 828 particles. We have 72 particles per layer, except for the topmost layer of the slab, which is made of three monoatomic, 3 atoms wide ledges. Our MD box at $T = 0.22T_m$ is shown in Fig. 3(a). Clearly, this configuration is more "stepped" than most real surfaces found in experiments. It was choosen in order to be close to the Au(423)

vicinal, where a previous MD study showed a very pronounced high–temperature faceting [22]. On the contrary, we find here that the stepped surface in Fig. 3(a) does not facet, but exhibits a different type of high–temperature instability. Particles in the top layer of the configuration shown in Fig. 3(a) perform collective motion on the surface, i.e. the whole step diffuses with a small exchange of particles with the underlying Au(111) substrate. A similar motion of single columns of gold atoms added on the Au(111) surface was observed by high–resolution electron microscopy [39]. In our simulation steps appear to attract each other and the two ledges merge into a larger one as shown in Fig. 3(b). At higher temperatures the third ledge joins them (Fig. 3(c)). While the flat Au(111) surface shows overheating, i.e. it melts about $\sim 100K$ above the bulk melting point for our potential [26], local melting and droplet formation does start at the edges of the large ledge below the bulk melting point (Fig. 3(d)).

In conclusion, the results presented in this Section show that, although the steps attract each other, the stepped Au(111) surface with monoatomic steps of the opposite sign does not exhibit the high–temperature faceting.

V. HIGH–TEMPERATURE BEHAVIOR OF THE Au(100) VICINALS

In experimental studies of crystals at high temperatures it was found that some orientations around (100) faces do not exhibit surface melting [11–17]. The existence of sharp edges, indicating the presence of high–temperature faceting for (100) vicinals, is not conclusive. Prompted by the unexplained high–temperature behavior around (100) faces we have also performed MD simulations for the Au(100)

vicinal surfaces.

The Au(100) surface reconstructs at low temperatures into an incommensurate hexagonal first–layer structure sitting on top of square bulk lattice. Recent X–ray diffraction studies [40,41] have shown that domains of distorted slightly rotated hexagonal reconstructed phase exist between 300K and 970K. This phase undergoes a transition at 970K into an unrotated distorted hexagonal phase which then disorders at 1170K. MD simulation for the Au(100) surface reconstruction showed that the optimal structure for our potential at $T = 0K$ is (34×5), and that all $(M \times 5)$, $28 \leq M \leq 40$, give a very small difference in the surface energy [28]. We are here interested in the high–temperature properties of the Au(100) surface since these properties determine the high–temperature morphology of the Au(100) vicinals. Recently, a MD simulation study of the high–temperature disordering of the Au(100) surface was performed [42]. It was found that the top layers disorder, but the Au(100) surface does not melt.

The Au(100) vicinal surfaces were also studied recently [29,35,37] and it was found that reconstruction induces the presence of favoured, particularly stable vicinals. MD simulation study (with the "glue" potential) for the $T = 0$ structure and energetics of gold vicinals has shown that on these "magic" vicinal surfaces, terraces contain an integer number of reconstruction cells [29]. It was found that the particularly stable Au(100) vicinals are: (11,1,1), (511) and (311). This result agrees with LEED [35] and scanning tunneling microscopy [37] studies of the Au(100) vicinals and periodic profiles. Non–magic vicinal surfaces facet into a suitable combination of magic vicinals and of flat (100). This reconstruction–induced faceting takes place at much lower temperatures than the faceting of the Au(111) vicinals described in

the Section III. Recently, reconstruction induced faceting for the (111) vicinals was studied at $T \sim 0.8T_m$ [36]. It was found that while some Au(111) vicinals are unstable and facet, vicinals of unreconstructed Pb(111) remain stable under the same conditions. Therefore the Au(111) vicinals show reconstruction–induced faceting as well as a high–temperature faceting. It is important to find out whether the Au(100) vicinals (which show the reconstruction induced faceting) also exhibit the high–temperature faceting.

We simulate here the Au(100) vicinal surfaces in the $(M,1,1)$, M odd, family. They consist of the (100) terraces, infinitely long along the $\langle 00\bar{1}\rangle$ direction and $(M+1)/2$ atoms wide along the $\langle 011\rangle$ direction. Due to the two–sublattice structure of the Au(100) surface the number of steps and terraces in periodically replicated MD boxes which represent the Au(100) vicinals must be multiple of 2. We choose here MD boxes with 2 steps and 2 terraces. MD trajectories for the magic Au(11,1,1) vicinal surface are shown in Figs. 4 and 5. This vicinal is misoriented by 6.7° from the (100) plane and the MD box consists of 752 particles. Fig. 5 shows that the high–temperature morphology of this surface does not change much with MD simulation time. Local melting fluctuations appears to take place, which make the two outermost layers very liquid–like close to T_m. We have also studied the Au(9 1 1) vicinal misoriented by 8° from the (100) plane, with 628 particles (shown in Fig. 6) and the Au(29,1,1) vicinal misoriented by 2.7°, with 1884 particles (shown in Figs. 7 and 8). The results for the Au(29,1,1) vicinal confirm MD study for the $T = 0$ surface energetics of the Au(100) vicinals [29]. This non–magic vicinal is unstable and, if prepared as an ideal sample at $T = 0$ (Fig. 7(a)), facets immediately (i.e. after a very short simulation time) even at low temperature (Fig. 7(b)). We expect

that the process of reconstruction induced faceting in our MD simulation at these low temperatures is not complete due to the limited diffusion. By contrast, the two other Au(100) vicinals we have studied, namely Au(11,1,1) and Au(911), are stable at low temperature, i.e. do not undergo reconstruction induced faceting. They eventually disorder with temperature as shown by Figs. 4–6, and steps disappear (but do not collapse) around $T \sim 0.6T_m$. At higher temperatures the surfaces deconstruct and several top layers become completely disordered. These surfaces do not exhibit proper surface melting close to the bulk melting point, in accordance with our results for the high–temperature properties of the Au(100) surface [42].

The results for the high–temperature morphology of the Au(100) vicinals in the $(M,1,1)$ family (M odd) show that these vicinals do not exhibit the high–temperature faceting. We are not able definitely to rule out the presence of sharp edges on crystal shape close to Au(100) in the surface melting temperature region, since there remains a possibility of high–temperature faceting for some other vicinal families not studied here. However, we feel this is an unlikely possibility. The reason is that lack of faceting for our (100) vicinal surfaces appears to be tied to the high–temperature disordering of the two uppermost layers of the flat (100) surface, a phenomenon which does not occur on the stable reconstructed (111). If this is true, then non–faceting at high temperatures is a property of (100) and will be true for all vicinals. As a counterexample, we can however recall the behavior of Si(111) vicinal surfaces. In experimental studies of the reconstruction induced faceting for the Si(111) vicinals it was found that some of them are unstable due to the $(7 \times 7) \rightarrow (1 \times 1)$ reconstruction on terraces and facet into the reconstructed flat (111) regions and regions with a high step density [33,34]. Still, one Si(111) vicinal

family is found not to facet under the same conditions, but to exhibit a tripling of the step height at the $(1 \times 1) \rightarrow (7 \times 7)$ transition [43]. Thus the reconstruction induced faceting for the Si(111) vicinals is strongly dependent on the interaction between the terrace reconstruction and the step orientation. Whether such dependence also exists for the high–temperature faceting, i.e. the study of the high–temperature morphology for other (100) and (111) vicinal families, must therefore be left for future work.

VI. CONCLUSIONS

We have shown by direct MD simulation that near the bulk melting temperature some Au(111) vicinal surfaces should be unstable and facet into flat (111) surface regions and tilted surface melted drops where surface diffusion is of a liquid type. This high–temperature faceting is induced by the surface melting anisotropy, i.e. the presence of both melting and non–melting faces on crystal shape in the vicinity of unstable vicinal surfaces. On the contrary, vicinal surfaces of the $(M,1,1)$ family (M odd), close to Au(100) do not facet near the bulk melting point. There steps disappear without collapsing well below the bulk melting temperature. High–temperature faceting is also absent for unlike monoatomic steps on the Au(111) surface. We expect similar high–temperature morphology for stepped surfaces of other fcc metals.

REFERENCES

[1] M. Wortis, in *Chemistry and Physics of Solid Surfaces*, vol. **7**, ed. R. Vanselow and R. Howe (Springer, Berlin, 1988), p. 367.

[2] H. van Beijeren and I. Nolden, in *Structure and Dynamics of Surfaces II*, ed. W. Schommers and P. Blanckenhagen (Springer, Berlin, 1987), p. 259.

[3] R. K. P. Zia, in *Progress in Statistical Mechanics*, ed. C. K. Hu (World Scientific, Singapore, 1988), p. 303.

[4] J. F. van der Veen, B. Pluis, and A. W. Denier van der Gon, in *Chemistry and Physics of Solid Surfaces*, vol. **7**, ed. R. Vanselow and R. Howe (Springer, Berlin, 1988), p.455.

[5] J. G. Dash, in *Proceedings of the Solvay Conference on Surface Science*, ed. by F. W. de Wette, p.142 (Springer, New York, 1988).

[6] E. Tosatti, in *The Structure of Surfaces II*, ed. J. F. van der Veen and M. A. van Hove (Springer, Berlin, 1988), p.535.

[7] R. Pandit, M. Schick, and M. Wortis, *Phys. Rev. B* **26**, 5112 (1982).

[8] A. C. Levi and E. Tosatti, *Surf. Sci.* **178**, 425 (1986).

[9] G. Bilalbegović, V. Privman, and N. M. Švrakić, *J. Phys. A* **22**, L833 (1989).

[10] C. Herring, *Phys. Rev.* **82**, 87 (1951).

[11] K. D. Stock and E. Menzel, *J. Cryst. Growth* **43**, 135 (1978).

[12] K. D. Stock and B. Grosser, *J. Cryst. Growth* **50**, 485 (1980).

[13] B. Pluis, A. W. Denier van der Gon, J. W. M. Frenken, and J. F. van der Veen, *Phys. Rev. Lett.* **59**, 2678 (1987).

[14] J. C. Heyraud, J. J. Métois, and J. M. Bermond, *J. Cryst. Growth* **98**, 355

(1989).

[15] J. J. Métois and J.C. Heyraud, *Ultramicroscopy* **31**, 73 (1989).

[16] J. J. Métois and J. C. Heyraud, *J. Phys. (France)* **50**, 3175 (1989).

[17] A. Pavlovska, K. Faulien, and E. Bauer, *Surf. Sci.* **221**, 233 (1989).

[18] P. Nozières, *J. Phys. (France)* **50**, 2541 (1989).

[19] P. Nozières, *Lecture given at the Beg-Rohu Summer School* (1989), unpublished.

[20] H. Löwen, *Surf. Sci.* **234**, 315 (1990).

[21] H. N. Yang, T. M. Lu, and G. C. Wang, *Phys. Rev. Lett.* **62**, 2148 (1989).

[22] G. Bilalbegović, F. Ercolessi, and E. Tosatti, *Surf. Sci.* **258**, L676 (1991).

[23] G. Bilalbegović, F. Ercolessi, and E. Tosatti, *Europhys. Lett.* **17**, 333 (1992).

[24] *Many-Atom Interactions in Solids*, eds. R. M. Nieminen, M. J. Puska, and M. J. Manninen (Springer, Berlin, 1990).

[25] F. Ercolessi, M. Parrinello, and E. Tosatti, *Phil. Mag. A* **58**, 213 (1988).

[26] P. Carnevali, F. Ercolessi, and E. Tosatti, *Phys. Rev. B* **36**, 6701 (1987).

[27] F. Ercolessi, S. Iarlori, O. Tomagnini, E. Tosatti, and X. J. Chen, *Surf. Sci.* **251/252** 645 (1991).

[28] F. Ercolessi, E. Tosatti, and M. Parrinello, *Phys. Rev. Lett.* **57**, 719 (1986).

[29] A. Bartolini, F. Ercolessi, and E. Tosatti, *Phys. Rev. Lett.* **63**, 872 (1989).

[30] J. V. Barth, H. Brune, G. Ertl, and R. J. Behm, *Phys. Rev. B* **42**, 9307 (1990) and references there.

[31] A. R. Sandy, S. G. J. Mochrie, D. M. Zehner, K. G. Huang, and D. Gibbs, *Phys. Rev. B* **43**, 4667 (1991) and references there.

[32] J. D. Gunton, M. San Miguel, and P. Sahni, in *Phase Transitions and Critical Phenomena*, Vol. 8, edited by C. Domb and J. L. Lebowitz, 267 (Academic,

London, 1983).

[33] R. J. Phaneuf and E. D. Williams, *Phys. Rev. Lett.* **58**, 2563 (1987).

[34] R. J. Phaneuf, E. D. Williams, and N. C. Bartelt, *Phys. Rev. B* **38**, 1984 (1988).

[35] M. Sotto and J. C. Boulliard, *Surf. Sci.* **214**, 97 (1989).

[36] G. Bilalbegović, F. Ercolessi, and E. Tosatti, *Europhys. Lett.* **18**, 163 (1992).

[37] H. P. Bonzel, U. Breuer, B. Voigtländer, and E. Zeldov, *Surf. Sci.*, to be published.

[38] M. Flytzani-Stephanopoulos and L. D. Schmidt, *Prog. Surf. Sci.* **9**, 83 (1979).

[39] J. O. Malm and J. O. Bovin, *Surf. Sci.* **200**, 67 (1988).

[40] S. G. J. Mochrie, D. M. Zehner, B. M. Ocko, and D. Gibbs, *Phys. Rev. Lett.* **64**, 2925 (1990).

[41] B. M. Ocko, D. Gibbs, K. G. Huang, D. M. Zehner, and S. G. J. Mochrie, *Phys. Rev. B***44**, 6429 (1991) and references there.

[42] G. Bilalbegović, F. Ercolessi, and E. Tosatti, to be published.

[43] R. J. Phaneuf and E. D. Williams, *Phys. Rev. B* **41**, 2991 (1990).

FIGURE CAPTIONS

Figure 1: Particle trajectories for the Au(534) vicinal of Au(111) at: (a) $T = 0.37T_m$, (b) $T = 0.99T_m$. Our trajectory plots refer to a time span of 10 ps, after an equilibration time up to several ns. Trajectories are observed along $(11\bar{2})$, and four $(11\bar{2})$ planes are overlapped in the pictures. The surface exhibits the high–temperature faceting.

Figure 2: Examples of fluctuations for the high–temperature faceting. The Au(534) surface is shown at $T = 0.99T_m$ after: (a) 1.8 ns, (b) 2.9 ns, (c) 3.6 ns, (d) 4.6 ns, (e) 5.4 ns, (f) 6.1 ns, (g) 6.4 ns, (h) 7.1 ns.

Figure 3: MD trajectories showing a slab with unlike steps on Au(111) at: (a) $T = 0.22T_m$, (b) $T = 0.73T_m$, (c) $T = 0.81T_m$, (d) $T = 0.99T_m$. Note the attraction of the steps and the absence of faceting.

Figure 4: Particle trajectories for the Au(11, 1, 1) vicinal of Au(100) at: (a) $T = 0.29T_m$, (b) $T = 0.66T_m$, (c) $T = 0.73T_m$. This surface gradually disorders with temperature.

Figure 5: The Au(11, 1, 1) vicinal surface at $T = 0.99T_m$ after: (a) 0.36 ns, (b) 0.71 ns, (c) 1.07 ns, (d) 1.43 ns. The surface does not exhibit the high–temperature faceting.

Figure 6: Particle trajectories for the Au(9 1 1) vicinal of Au(100) at: (a) $T = 0.81T_m$, (b) $T = 0.92T_m$, (c) $T = 0.95T_m$, (d) $T = 0.99T_m$. Liquid–like diffusion at high–temperatures is located mainly in the two topmost layers.

Figure 7: Snapshot of the MD slab for the Au(29,1,1) vicinal of Au(100). Side view of two MD boxes is shown at: (a) $T = 0$ (ideal sample), (b) $T = 0.15T_m$. This

unstable vicinal surface exhibits reconstruction induced faceting at very low temperatures.

Figure 8: Particle trajectories for the Au(29, 1, 1) vicinal at: (a) $T = 0.81T_m$, (b) $T = 0.95T_m$, (c) $T = 0.99T_m$. After undergoing reconstruction induced faceting at low temperatures (see Fig. 7) the two topmost layers disorder at high temperatures.

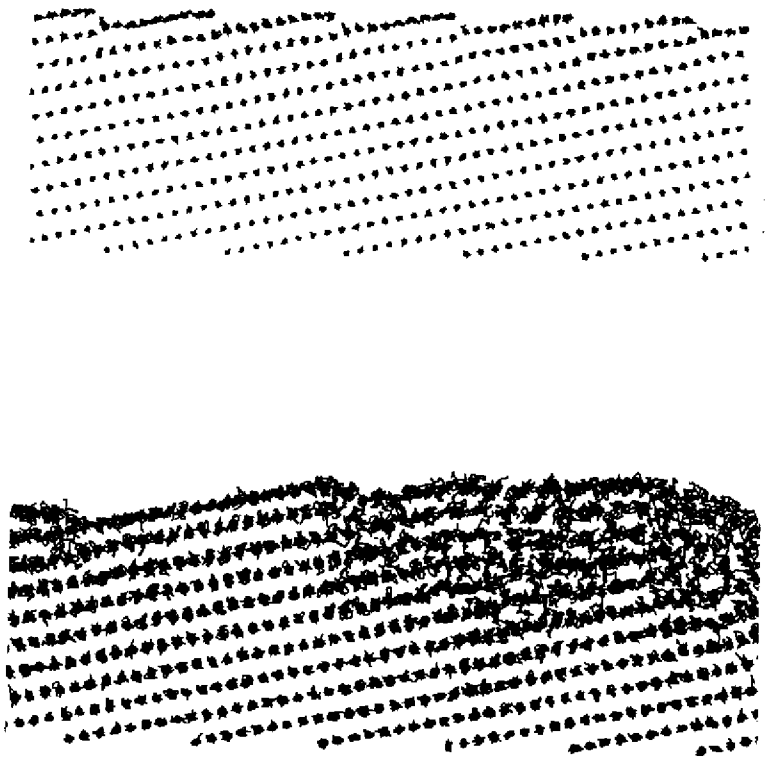

Fig.1

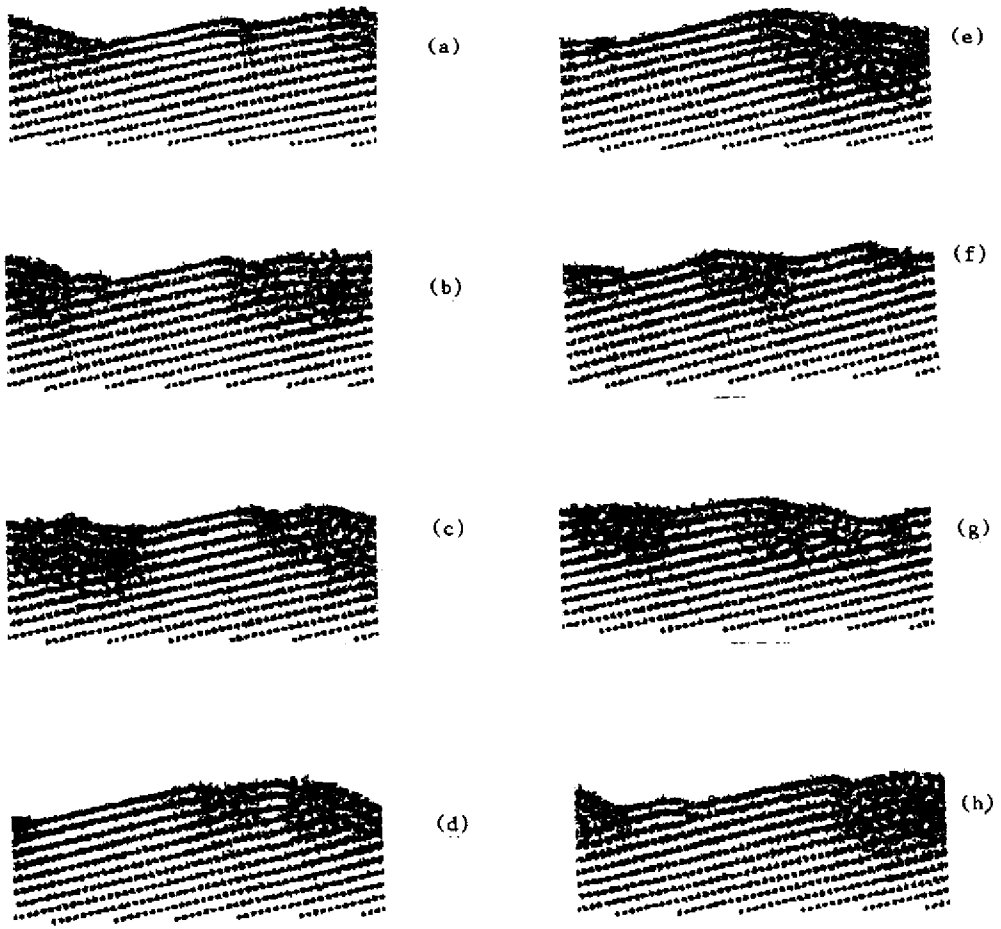

Fig.2

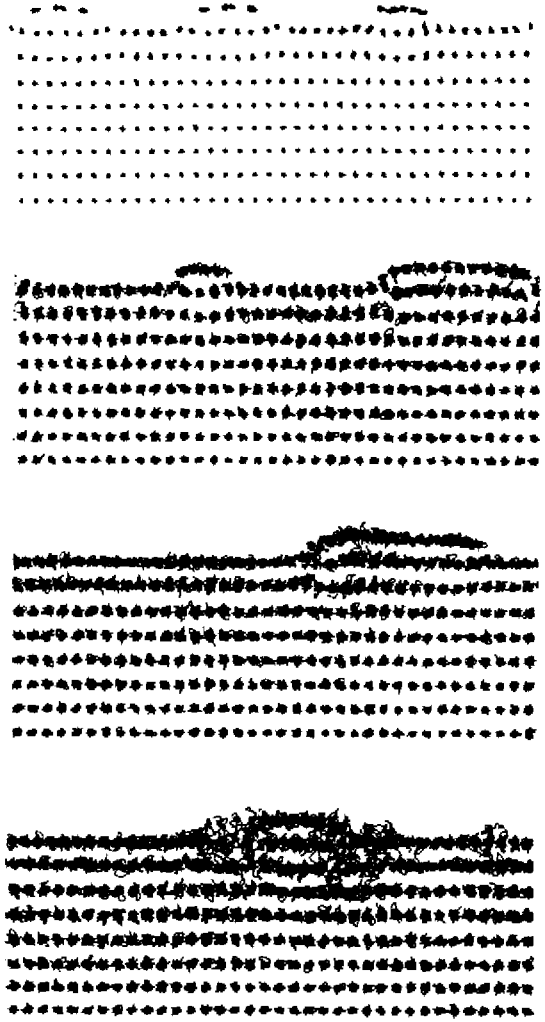

Fig.3

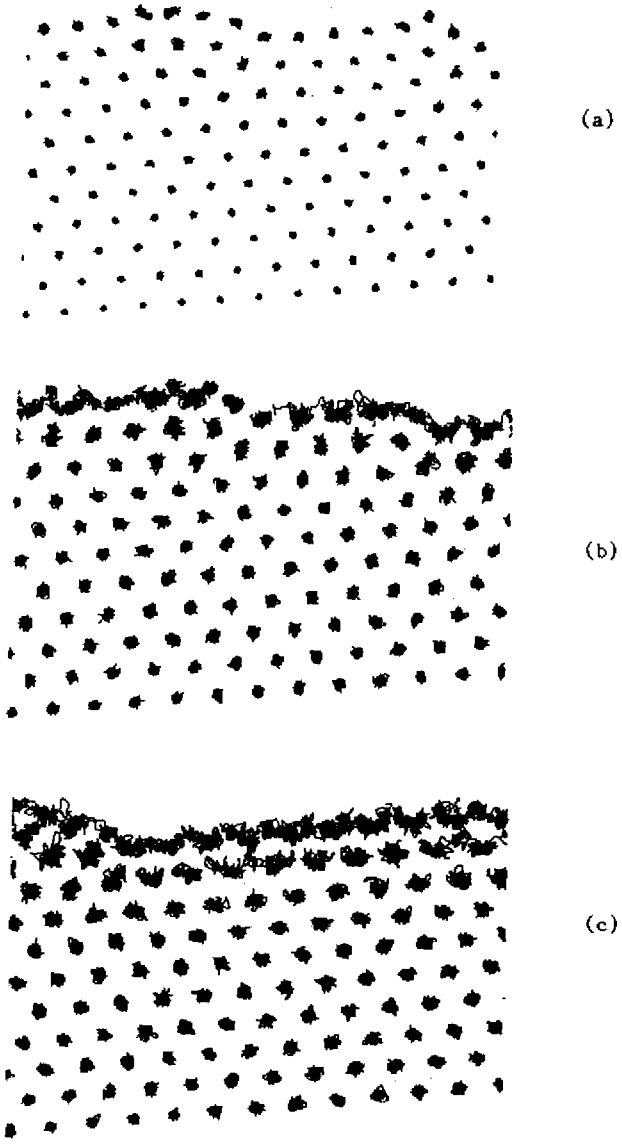

Fig.4

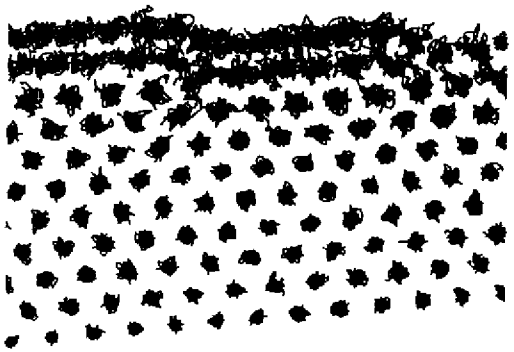

(a)

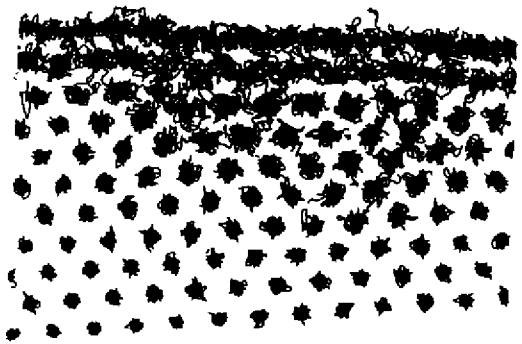

(b)

Fig.5

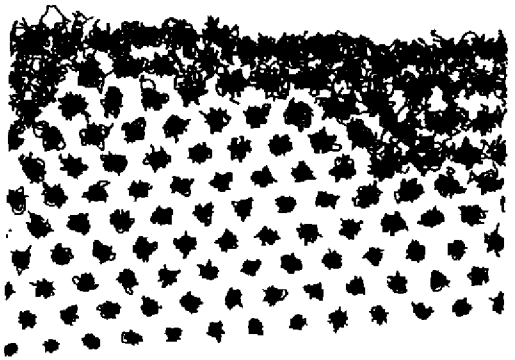

(c)

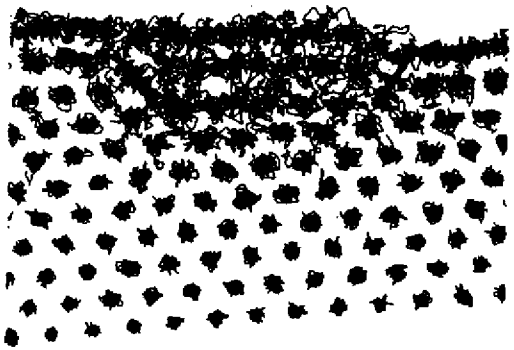

(d)

Fig.5

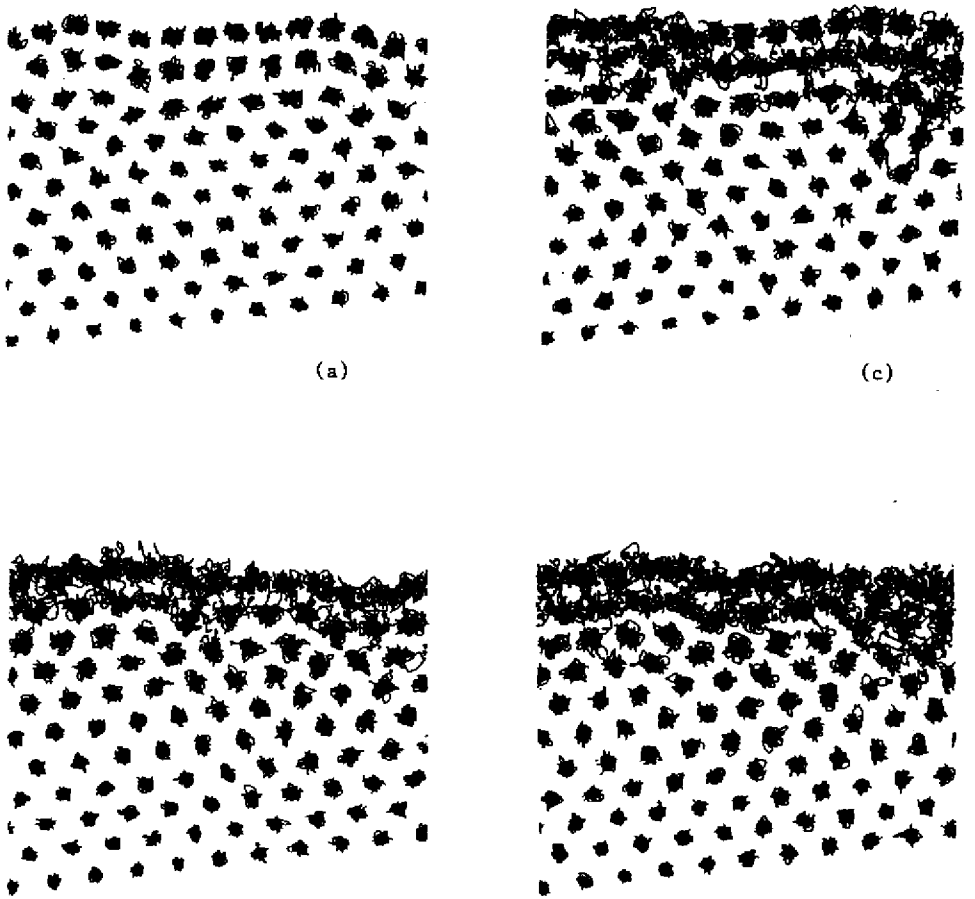

Fig.6

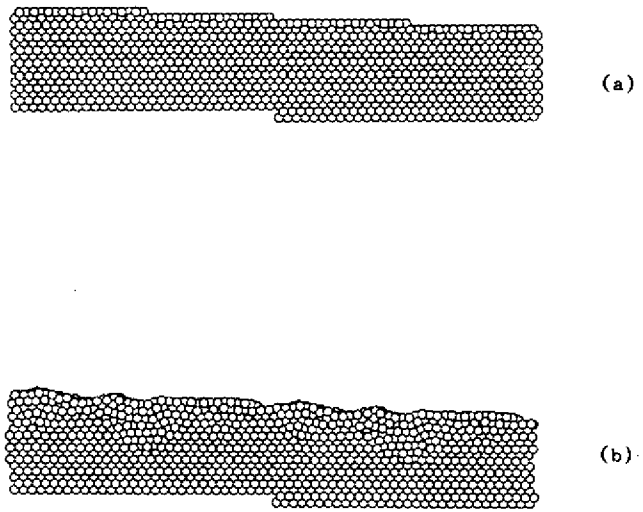

Fig.7

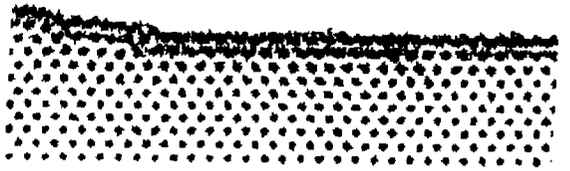

(a)

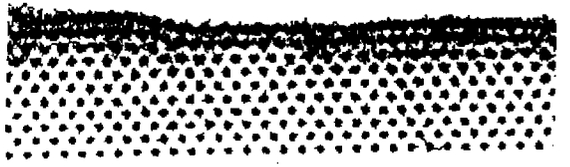

(b)

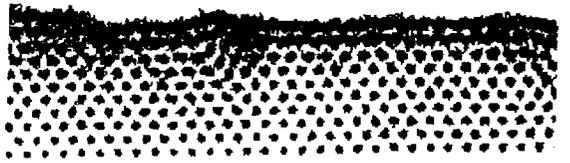

(c)

Fig.8